TIME-OPTIMAL CONTROL OF A PARTICLE IN A DIELECTROPHORETIC SYSTEM

Dong Eui Chang Nicolas Petit Pierre Rouchon

CAS, Ecole des Mines de Paris
60, bd. Saint-Michel, 75272 Paris, CEDEX 06, France

Abstract: We study the time-optimal control of a particle in a dielectrophoretic system. This system consists of a time-varying non-uniform electric field which acts upon the particle by inducing a dipole moment within it. The interaction between the dipole and the electric field generates the motion of the particle. The control is the voltage on the electrodes which creates the electric field. Such systems have wide applications in bio/nanotechnology. In regard to time-optimal control, we address the issue of existence and uniqueness of optimal trajectories.

Keywords: time-optimal control, biotechnology, nanotechnology, dielectrophoresis

1. INTRODUCTION

We consider the motion of a neutrally-buoyant and neutrally-charged particle on an invariant line in a chamber filled with fluid flowing at low Reynolds number and with a parallel electrode array at the bottom of the chamber; see Figure 1. A force is created by the interaction between a non-uniform electric field and the dipole moment induced in the particle. The resultant motion is called *dielectrophoresis* (DEP); see (Pohl, 1978). We are interested in the time-optimal control of this system which can be described, after a nonlinear change of coordinates, by

$$\dot{x} = yu + \alpha u^2 \tag{1}$$
$$\dot{y} = -cy + u. \tag{2}$$

The state $(x, y) \in \mathbb{R}^2$ and the single control u satisfy

$$x(0) = \text{ given}, \quad y(0) = 0, \tag{3}$$
$$x(t_f) = \text{ given}, \quad y(t_f) = \text{ free}, \tag{4}$$
$$|u| \leq 1 \tag{5}$$

where the parameters α and c satisfy

$$\alpha < 0, \quad c > 0. \tag{6}$$

Variable x describes the displacement of the particle. Variable y describes the exponentially-decaying part of the induced dipole moment. Voltage u is given on every other electrode and $(-u)$ on the others. Parameters α and c depend on the permittivities and conductivities of the particle and the fluid medium. Dielectrophoresis has wide applications in bio/nanotechnology, in particular, in the separation of bio/nano-particles (Hughes, 2002; Jones, 1995). We here address the case of a single particle to underline key features of DEP such as the dipole induction and the boundary control. We hope that this will invite control researchers to the application of DEP systems.

2. OVERVIEW OF MAIN RESULTS

Time optimal trajectories satisfy the following dynamics:

$$\dot{x} = yu + \alpha u^2 \tag{7}$$
$$\dot{y} = -cy + u \tag{8}$$
$$\dot{\lambda} = c\lambda - u \tag{9}$$

with conditions (3) – (5) and

$$\lambda(0) = \lambda_0 = \text{to be found}, \quad \lambda(t_f) = 0 \tag{10}$$

where

$$u(t) = \arg\max_{|v|\le 1} \tilde{H}(y(t), \lambda(t), v)$$

with

$$\tilde{H}(y, \lambda, v) = \alpha u^2 + (y+\lambda)u - cy\lambda. \tag{11}$$

See (23) for the optimal control u.

When $x_f < x(0)$, there are no Lebesgue measurable time-optimal control functions resulting in $x(t_f) = x_f$ even though x_f is reachable.

We now consider the case of $x_f > x_0$. Time-optimal control law exists if and only if the parameters, α and c satisfy $(1+\alpha c) > 0$, which is assumed in the following of this section. Let

$$\Lambda = (-2\alpha\sqrt{1+\alpha c}, -2\alpha\sqrt{(1+\alpha c)/(-\alpha c)}) \tag{12}$$

for $(1+2\alpha c) \le 0$, and

$$\begin{aligned}\Lambda &= \Lambda_1 \cup \Lambda_2 \\ &= (-2\alpha\sqrt{1+\alpha c}, -2\alpha) \cup [-2\alpha, 1/c)\end{aligned} \tag{13}$$

for $(1+2\alpha c) > 0$. For the sake of convenience, let us define three sentences as follows:

- P1 $:= [(1+2\alpha c) > 0] \wedge [\lambda_0 \in \Lambda_1]$,
- P2 $:= [(1+2\alpha c) > 0] \wedge [\lambda_0 \in \Lambda_2]$,
- Q $:= [(1+2\alpha c) \le 0] \wedge [\lambda_0 \in \Lambda]$

where $\wedge$ is the logical connective, AND. Let us define a strictly increasing onto function $X_1 : \Lambda$ *rightarrow*$(0,\infty)$ by

$$X_1(\lambda_0) = \begin{cases} \text{equation (24)} & \text{if P1} \vee \text{Q}, \\ \text{equation (26)} & \text{if P2} \end{cases}$$

where $\vee$ is the logical connective, OR. Let us define another function T_1 on Λ by

$$T_1(\lambda_0) = \begin{cases} \text{equation (30)} & \text{if P1} \vee \text{Q}, \\ \text{equation (31)} & \text{if P2.} \end{cases}$$

Classically, we call a trajectory of (7) – (9) satisfying (3) – (5) and (10), an *extremal*. Let us call an arc of an extremal a *basic arc* if the projection of the arc onto the $y\lambda$-plane starts from $0 \times \Lambda$ (resp. $0 \times (-\Lambda)$) and ends on $\Lambda \times 0$ (resp. $(-\Lambda) \times 0$), going through the first (resp. third) quadrant of the $y\lambda$-plane. We call an extremal an *n-shot extremal* with $n \in \mathbb{N}$ if the maximum number of basic arcs in the extremal is n.

To decompose extremals into finite arcs when [P1 $\vee$ Q], let us introduce some notations. An arc with the linear control $u = (y+\lambda)/(-2\alpha)$ on a time interval of length $\Delta t_{AB}(\lambda_0)$ in (27), is denoted by $\gamma_{\mathrm{L}}^{\lambda_0}$. Let $\gamma_+^{\lambda_0}$ (resp. $\gamma_-^{\lambda_0}$) denote an arc with $u = 1$ (resp. $u = -1$) in a time interval of length $\Delta t_{BC}(\lambda_0)$ in (29). Define two arcs $\Gamma_\pm^{\lambda_0}$ by the concatenation

$$\Gamma_\pm^{\lambda_0} = \gamma_L^{\lambda_0} \star \gamma_\pm^{\lambda_0} \star \gamma_L^{\lambda_0} \tag{14}$$

where the concatenation $\star$ is defined such that the leftmost one comes first and the rightmost one comes last and the concatenation curve is always a continuous curve. An arc with the linear control $u = (y+\lambda)/(-2\alpha)$ is called an *idling arc* if its projection (y, λ) starts from the positive (resp., negative) y-axis, goes through the fourth (resp., second) quadrant in the $y\lambda$-plane, and finally ends on the negative (resp., positive) λ-axis. An idling arc is denoted by γ_{idling}; see (b) of Figure 3. Its duration is T_{idling} in (32). Hence, when [P1 $\vee$ Q], we can express n-shot extremals as $\Gamma_\pm^{\lambda_0,n}$, $n \in \mathbb{N}$ which is defined as follows:

$$\Gamma_\pm^{\lambda_0,1} = \Gamma_\pm^{\lambda_0};$$

$$\Gamma_\pm^{\lambda_0,k} = \begin{cases} \Gamma_\pm^{\lambda_0,k-1} \star \gamma_{\text{idling}} \star \Gamma_\mp^{\lambda_0} & \text{if } k \text{ is even}, \\ \Gamma_\pm^{\lambda_0,k-1} \star \gamma_{\text{idling}} \star \Gamma_\pm^{\lambda_0} & \text{if } k \text{ is odd} \end{cases}$$

for $k \ge 2$ with

$$\lambda(0) = \pm\lambda_0.$$

Let us now talk about the existence and uniqueness of optimal trajectories. If $(1+2\alpha c) > 0$, there exist exactly two time-optimal trajectories for a given $x_f > x(0)$, and they are basic arcs. Here is the procedure of constructing them:

1. Find $\lambda_0 = X_1^{-1}(x_f - x(0)) \in \Lambda$,
2. Set $\lambda(0) = \pm\lambda_0$,
3. The minimum time cost is $T_1(\lambda_0)$ and the optimal trajectories γ_{opt} are

$$\gamma_{\text{opt}} = \begin{cases} \Gamma_\pm^{\lambda_0} & \text{if P1}, \\ \text{basic arc with } u = \pm 1 & \text{if P2.} \end{cases}$$

If $(1+2\alpha c) \le 0$, we do not have any general proof of the uniqueness of optimal control. However, we have a finite procedure of finding all optimal control laws for a given $x_f > x(0)$ as follows:

1. Define two sequences, for $k \in \mathbb{N}$,

$$\lambda_{0,k} = X_1^{-1}\left(\frac{x_f - x(0)}{k}\right),$$
$$T_k = k\, T_1(\lambda_{0,k}) + (k-1)T_{\text{idling}}$$

2. Find $n = \arg\min_k \{T_k : k \in \mathbb{N}\}$ (it always exists and is less than $1 + (T_1/T_{\text{idling}})$),
3. Set $\lambda(0) = \pm\lambda_{0,n}$,
4. The minimum time cost is T_n and the corresponding optimal trajectories are $\Gamma_\pm^{\lambda_0,n}$.

If there are j integers in step 2 to give the minimum time, then there are exactly $2j$ time-optimal trajectories. We remark that each basic arc in the k-shot extremal $\Gamma_\pm^{\lambda_{0,k},k}$ equally contributes $(x_f - x(0))/k$ to the increment of x and the idling arcs in between make no contributions.

3. DERIVATION OF DYNAMICS

We briefly derive the dynamics in (1) and (2), and explain the conditions on the state and parameters in (3) – (6); see (Chang *et al.*, 2003) for more detail. Consider a neutrally charged particle in a chamber with a fluid medium and a parallel electrode array at the bottom as in (a) of Figure 1 where d_1 is the width of each electrode, and d_2 is the length of the gap between two electrodes. As the electrodes are long enough compared with the size of particles, we may assume that there are infinite number of infinitely long electrodes. Due to this symmetry, we will consider the motion of the particle in the vertical plane as in (b) of Figure 1. Let $(q, p) \in \mathbb{R}^2$ be the coordinates in (b)

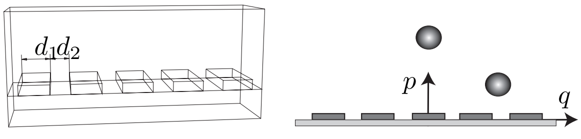

(a) (b)

Fig. 1. The dielectrophoretic system is a chamber filled with a fluid medium where there is a parallel array of electrodes at the bottom.

of Figure 1. We give the boundary voltage

$$V_{\text{bd}}(t) = V_0 \cdot u(t), \quad |u(t)| \leq 1$$

on every other electrode and $(-V_{\text{bd}}(t))$ on the others. This creates potential $V(q, p, t)$ in $\{p \geq 0\}$. The electric field $\mathbf{E}(q, p, t)$ in $\{p \geq 0\}$ is given by

$$\mathbf{E}(q, p, t) = -\nabla V(q, p, t).$$

This electric field induces a dipole moment, $\mathbf{m}$, on a single-layered spherical particle as follows:

$$\mathbf{m}(q, p, t) = g(t) * \mathbf{E}(q, p, t)$$

where $*$ denotes time-convolution and the Laplace transform $G(s)$ of the (transfer) function $g(t)$ is given by

$$G(s) = a + \frac{b}{s + c}$$

where

$$a = 4\pi r^3 \epsilon_m (\epsilon_p - \epsilon_m)/(\epsilon_p + 2\epsilon_m),$$

$$b = a\left(\frac{\sigma_p - \sigma_m}{\epsilon_p - \epsilon_m} - \frac{\sigma_p + 2\sigma_m}{\epsilon_p + 2\epsilon_m}\right), \tag{15}$$

$$c = (\sigma_p + 2\sigma_m)/(\epsilon_p + 2\epsilon_m) \tag{16}$$

where r is the radius of the particle, ϵ_p (resp., ϵ_m) is the permittivity of the particle (resp., medium) and σ_p (resp., σ_m) is the conductivity of the particle (resp., medium). The interaction between the electric field and the induced dipole moment creates a force $\mathbf{F}_{\text{dep}}$. It is called *dielectrophoretic force* and given by

$$\mathbf{F}_{\text{dep}}(q, p, t) = (\mathbf{m}(q, p, t) \cdot \nabla)\mathbf{E}(q, p, t).$$

As the vertical motion of particles in the whole chamber can be practically represented by that of particles on the p axis, we are interested in the motion of particles on the p axis. One can check that the dielectrophoretic force on the p axis is along this axis. This vertical dielectrophoretic force on the p axis is denoted by $F_{\text{dep}}(p, t)$. It is of the form

$$F_{\text{dep}}(p, t) = F(p)u(t)(g * u)(t)$$

with $F(p) \leq 0$ on $p \geq 0$, $\lim_{p\to\infty} F(p) = 0$, and $F(p) = 0$ only at $p = 0$; see (Chang *et al.*, 2003).

Let us assume that *the particle is neutrally buoyant and the medium fluid flows at low Reynolds number.* Thus, the gravitational force and the buoyant force cancel and the inertial term $m\ddot{p}$ is ignorable. The only forces on the particle are the drag and the DEP force. Hence, the motion of the particle on the p axis can be described by

$$f\,\dot{p} + F(p)u(t)(g * u)(t) = 0. \tag{17}$$

where $f > 0$ is the drag constant.

We assume that b in (15) is nonzero, which generically holds. Then equations (1) and (2) come from (17) where x and y are defined by

$$x = \int_{\epsilon}^{p} \frac{-f}{b\,F(z)}\mathrm{d}z; \quad Y(s) = \frac{1}{s + c}U(s) \tag{18}$$

for $p \geq \epsilon$ where ϵ is a positive number and $Y(s)$ and $U(s)$ are the Laplace transforms of $y(t)$ and $u(t)$, and α is defined by

$$\alpha = a/b.$$

If a particle is close to the electrode, then additional physical/chemical forces other than the DEP force start to appear in the dynamics (Hughes, 2002; Pohl, 1978), so the parameter ϵ in (18) defines the region where the dynamics (17) is valid. Physically, y is the exponentially induced part of the dipole moment, so we have the initial condition $y(0) = 0$. As we are not interested in the final state of the induced dipole moment, we have $y(t_f) = $ free.

Depending on the sign of b, the original region $\{p \geq \epsilon\}$ is mapped to $\{x \geq 0\}$ or $\{x \leq 0\}$. However, in this paper, we ignore the state constraint on x, allowing for x on the whole real line. In a future publication, we will address the state constraint on x.

We also make the following assumption on the signs of parameters α and c

$$\alpha < 0, \quad c > 0.$$

Assumption $c > 0$ is imposed by physics; see (16). However, condition $\alpha < 0$ is for convenience. The case of $\alpha \geq 0$ can be treated in the similar manner.

4. MAIN DISCUSSION

4.1 Non-existence of optimal control for $x_f < x(0)$.

We will show that there are no time-optimal (Lebesque) measurable controls for $x_f < x(0)$

even though x_f is reachable. For a $T > 0$, let us define a sequence of functions $\{u_n^T : [0, T] \to \pm 1\}$ as follows:

$$u_n^T(t) = \mathrm{sign}(\sin(2\pi n t/T)), \quad n \in \mathbb{N}. \qquad (19)$$

Lemma 1. Let f be a continuous function on $[0, T]$. Then, $\lim_{n \mapsto \infty} \int_0^t f \cdot u_n^T = 0$, uniformly in $t \in [0, T]$.

The substitution of u from (2) to (1) yields

$$\dot{x} = y\dot{y} + cy^2 + \alpha u^2.$$

For any $T > 0$ we have

$$x(T) - x(0) = \frac{1}{2} y(T)^2 + c \int_0^T y^2 + \alpha \int_0^T u^2 \geq \alpha T \qquad (20)$$

where the last inequality holds by (5). This implies that in the time interval $[0, T]$, the negatively farthest reachable point is at best $x(0) + \alpha T$. Let (x_n, y_n) be the solution to (1) and (2) on $[0, T]$ with control u_n^T in (19). By Lemma 1, (20), and the definition of u_n^T, one can show

$$\lim_{n \to \infty} (x_n(T) - x(0)) = \alpha T.$$

We have constructed a sequence $\{u_n^T\}$ of control laws such that the corresponding $\{x_n(T)\}$ converges to the infimum of the reachable points of x. However, the sequence of functions $\{u_n^T\}$ does not converge to a measurable function. One can prove that *for $x_f < x(0)$, the infimum of the reachable time is $T = (x(0) - x_f)/(-\alpha)$, but there are no time-optimal (Lebesgue) measurable controls to reach x_f in time T.* We remark that for $x_f = x(0)$, control $u = 0$ with $t_f = 0$ is trivially the time-optimal control. Hence, *in the rest of the paper, we only consider the case of $x_f > x(0)$.*

4.2 Pontryagin maximum principle, Necessary condition on parameters and Discrete symmetry.

We derive, from the Pontryagin Maximum Principle (PMP), necessary conditions for time-optimal trajectories. Let us define the PMP Hamiltonian, H, for the time-optimal control as follows (Pontryagin *et al.*, 1962):

$$H(x, y, \lambda_x, \lambda_y, u) = \lambda_x \alpha u^2 + (\lambda_x y + \lambda_y) u - c y \lambda_y$$

where (λ_x, λ_y) is the vector dual to (x, y). Let

$$H^\circ(x, y, \lambda_x, \lambda_y) = \max_{|u| \leq 1} H(x, y, \lambda_x, \lambda_y, u).$$

Consider system (1), (2) with conditions (3) – (5) and (6). Let $u(t)$ be a time-optimal control and $(x(t), y(t))$ be the corresponding trajectory. Then, by the PMP, it is necessary that there exists a continuous vector $(\lambda_x(t), \lambda_y(t))$, which is not identically zero, such that

$$\dot{x} = yu + \alpha u^2; \ \dot{y} = -cy + u,$$
$$\dot{\lambda}_x = 0; \ \dot{\lambda}_y = c\lambda_y - \lambda_x u. \qquad (21)$$

Additionally, the following must be satisfied:

1. $u(t) = \arg \max_{|v| \leq 1} H(x(t), y(t), \lambda_x(t), \lambda_y(t), v)$,
2. $H^\circ(t) = \text{constant} \geq 0$,
3. $\lambda_y(t_f) = 0$ (transversality condition). (22)

As $\dot{\lambda}_x = 0$ in (21), $\lambda_x(t)$ is constant in time. We consider the three different cases; $\lambda_x = 0$, $\lambda_x < 0$ and $\lambda_x > 0$.

A simple integration of (21) with the transversality condition (22) implies that $\lambda_x = 0$ implies $\lambda_y(t) \equiv 0$. Hence, there cannot be any optimal trajectories with $\lambda_x = 0$ because the vector (λ_x, λ_y) cannot be identically zero by the PMP.

In the case of $\lambda_x < 0$, one can show, by simple computation, that no extremals satisfy both the initial condition $y(0) = 0$ and the transversality condition (22). Hence, there exist no optimal trajectories with $\lambda_x < 0$, either.

We now assume that $\lambda_x > 0$. Let

$$\lambda = \lambda_y / \lambda_x; \quad \tilde{H}(y, \lambda, u) = H / \lambda_x.$$

Then equation (21) is replaced by (9), giving us the set of equations (7) – (9). As $\alpha < 0$, the control u maximizing $\tilde{H}$ (or equivalently H) is given by

$$u = \begin{cases} +1 & \text{if } y + \lambda > -2\alpha, \\ \dfrac{y + \lambda}{-2\alpha} & \text{if } |y + \lambda| \leq -2\alpha, \\ -1 & \text{if } y + \lambda < -2\alpha. \end{cases} \qquad (23)$$

The (y, λ) dynamics with the control (23) have three qualitatively different phase portraits depending on the sign of $(1 + \alpha c)$. For example, the origin $(y, \lambda) = (0, 0)$ becomes a saddle, a degenerate equilibrium, and a center, respectively if $(1 + \alpha c)$ is negative, zero and positive, respectively. A simple but thorough phase portrait analysis shows – we omit the detail – that when $(1 + \alpha c) < 0$ or $(1 + \alpha c) = 0$, there are no trajectories satisfying the initial condition $y(0) = 0$ and the final condition $\lambda(t_f) = 0$ (equivalently, $\lambda_y(t_f) = 0$). Hence, time-optimal trajectories exist only when

$$1 + \alpha c > 0$$

which is assumed in the following of the paper. In this case, the dynamics of (y, λ) have two qualitatively different phase portraits depending on

$$(1 + 2\alpha c) \leq 0, \text{ or } (1 + 2\alpha c) > 0.$$

The portraits are given in Figure 2. A big difference between the two is whether the intersection of the positive λ-axis and the switching line $y + \lambda = -2\alpha$ is above or below $(0, 1/c)$.

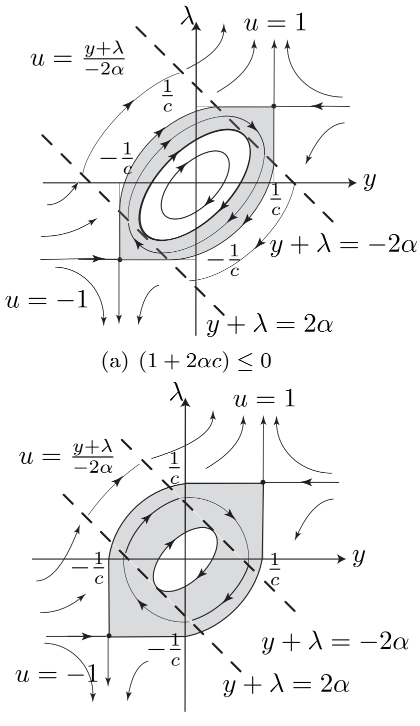

(a) $(1+2\alpha c)\le 0$

(b) $(1+2\alpha c)>0$

Fig. 2. The phase portrait in the $y\lambda$-plane when $\lambda_x>0$ and $(1+\alpha c)>0$. Depending on the sign if $(1+2\alpha c)$, point $(0,-2\alpha)$ is above or below point $(0,1/c)$ on the λ axis.

We now discuss about the discrete symmetry in the phase portraits. Let us define three reflections, $S_i, i=1,2,3$ as follows:

$$
\begin{aligned}
&S_1(x,y,\lambda)=(x,\lambda,y),\\
&S_2(x,y,\lambda)=(x,-\lambda,-y),\\
&S_3(x,y,\lambda)=S_1\circ S_2(x,y,\lambda)=(x,-y,-\lambda).
\end{aligned}
$$

Denoting by Z_{L} the dynamics in (7) – (9) with the linear control $u=(y+\lambda)/(-2\alpha)$, one can check

$$S_i\circ Z_{\mathrm{L}}=-Z_{\mathrm{L}}\circ S_i,\quad i=1,2.$$

The linear vector field, Z_{L}, is invariant under reflections, S_1 and S_2, up to the time-reversal. In (a) of Figure 3 the duration Δt_{AB} from A to B along the trajectory with $u=(y+\lambda)/(-2\alpha)$ in the $y\lambda$-plane equals $\Delta t_{S_i(B)S_i(A)}$, $i=1,2$. The corresponding increments in x satisfy

$$\Delta x_{AB}=-\Delta x_{S_i(B)S_i(A)},\quad i=1,2.$$

This implies that in the white region surrounded by the shaded region in Figure 2 there cannot be any optimal trajectories because any orbits starting from the λ axis and ending at the y axis can be decomposed into parts, each of which is invariant under S_1 or S_2. This implies $\Delta x=0$. However, we already know what the time-optimal control is for $\Delta x=0$. It is $u=0$ with $t_f=0$. *Therefore, all time-optimal trajectories are contained in the shaded region because only the extremals in the shaded region can satisfy* $y(0)=0$ *and* $\lambda(t_f)=0$.

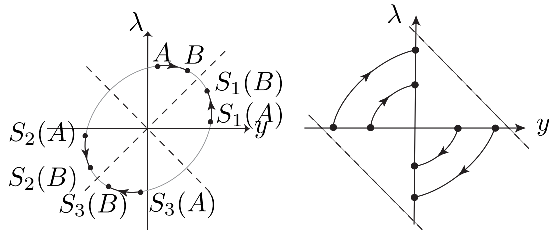

(a) Symmetries (b) Idling arcs

Fig. 3. (a) Discrete symmetries in the linear region. (b) Idling arcs.

Let us consider symmetry S_3. Let Z be the vector field in (7) – (9) with the control u in (23). Then we have $S_3\circ Z=Z\circ S_3$, which implies $\Delta t_{AB}=\Delta t_{S_3(A)S_3(B)}$ and $\Delta x_{AB}=\Delta x_{S_3(A)S_3(B)}$ in (a) of Figure 3.

4.3 *Construction of X_1, T_1 and T_{idling}.*

We call the part of the shaded region in Figure 2 lying in the first quadrant *the basic region.* We include the part on the y-axis and the λ-axis but we exclude the boundary of the shaded region which is in the first quadrant. Let Λ denote the open interval on the λ axis of the basic region. It is given in (12) and (13). For example, (12) comes from

$$
\begin{aligned}
\Lambda=\{\lambda\in\mathbb{R}_+\mid M(-\alpha,-\alpha)&<M(0,\lambda)\\
&<M(-(1+2\alpha c)/c,1/c)\}
\end{aligned}
$$

where M is the Hamiltonian $\tilde{H}$ in (11) with $u=(y+\lambda)/(-2\alpha)$. One can see that the arc of an extremal contained in the basic region is a basic arc, which is defined in § 2.

Let us construct a map X_1 on Λ, which measures the increment of x along a basic arc starting with $\lambda(0)\in\Lambda$. We show the construction in the case of $(1+2\alpha c)>0$ only, as the other case can be done similarly. When $(1+2\alpha c)>0$, we can decompose Λ into Λ_1 and Λ_2 as in (13). The basic arc with $\lambda(0)\in\Lambda_1$ is exactly $\Gamma_+^{\lambda(0)}$ defined in (14), which corresponds to $ABCD$ in Figure 4. The basic arc with $\lambda(0)\in\Lambda_2$ corresponds to FG in Figure 4. Suppose $\lambda(0)=\lambda_0\in\Lambda_1$. By the S_1-symmetry,

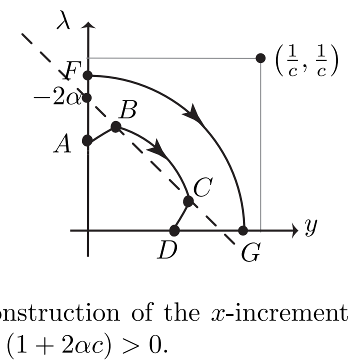

Fig. 4. Construction of the x-increment map X_1 when $(1+2\alpha c)>0$.

the x-increment along AB and along CD cancel each other out, so $X_1(\lambda_0)$ is the x-increment along BC, which can be computed as follows:

$$X_1(\lambda_0) = \frac{1}{c}\left[-2\alpha - 2y_C(\lambda_0) + \left(\alpha + \frac{1}{c}\right)\ln\left(\frac{1+2\alpha c + cy_C(\lambda_0)}{1-cy_C(\lambda_0)}\right)\right] \quad (24)$$

where y_B and y_C are the y-coordinates of points B and C and are given by

$$y_B(\lambda_0) = -\alpha - \sqrt{\alpha^2 + (\lambda_0^2 - 4\alpha^2)/(-4\alpha c)},$$
$$y_C(\lambda_0) = -y_B(\lambda_0) - 2\alpha. \quad (25)$$

In the similar way, one can compute $X_1(\lambda_0)$ with $\lambda_0 \in \Lambda_2$, which is given by

$$X_1(\lambda_0) = \frac{1}{c}\left[-\lambda_0 - \frac{(1+\alpha c)\ln(1-c\lambda_0)}{c}\right]. \quad (26)$$

Regarding X_1 in (24) as a function of y_C, one can check $dX_1/dy_C > 0$ on Λ_1. As y_C in (25) is a strictly increasing function of λ_0, it follows that X_1 is strictly increasing on Λ_1. By computing $dX_1/d\lambda_0 > 0$, one can show that X_1 in (26) is also strictly increasing on Λ_2. Thus, X_1 *is a strictly increasing function on* Λ. One can also show

$$X_1(\Lambda) = (0, \infty).$$

Let T_1 be the time duration of basic arcs with $\lambda(0) \in \Lambda$, so it becomes a function on Λ. We only show its construction in the case of $(1+2\alpha c) > 0$ for the space limit. Consider a basic arc with $\lambda_0 \in \Lambda_1$. It is of form $\Gamma_+^{\lambda_0}$, e.g., arc $ABCD$ in Figure 4. By the S_1-symmetry, the duration of AB equals that of CD, which is denoted by Δt_{AB} and given by

$$\Delta t_{AB}(\lambda_0) = \frac{1}{\omega} \times \sin^{-1}(-2\alpha\omega y_B(\lambda_0)/\lambda_0) \quad (27)$$

where

$$\omega = \sqrt{c(1+\alpha c)/(-\alpha)} > 0. \quad (28)$$

A simple integration yields the duration, Δt_{BC} of the arc BC, which is given by

$$\Delta t_{BC}(\lambda_0) = \frac{1}{c}\ln\left(\frac{1-cy_B(\lambda_0)}{1-cy_C(\lambda_0)}\right). \quad (29)$$

Hence, T_1 on Λ_1 is given by

$$T_1 = 2\Delta t_{AB} + \Delta t_{BC}. \quad (30)$$

By a direct integration in the similar way, one can show that T_1 on Λ_2 is given by

$$T_1(\lambda_0) = (-1/c) \times \ln(1 - c\lambda_0). \quad (31)$$

Recall the definitions of idling arcs and the idling time in § 2; see also (b) of Figure 3. The name of idling arcs comes from the fact that they do not contribute any increments in x by the S_1- and S_2-symmetry. One can compute the idling time, T_{idling}, as follows:

$$T_{\text{idling}} = (1/\omega) \times \sin^{-1}(-2\alpha\omega) \quad (32)$$

with ω in (28). Notice that the idling time is independent of the coordinates of the initial points on the y-axis.

4.4 *Existence and uniqueness of optimal trajectories.*

We can classify extremals with $k \in \mathbb{N}$ defined in § 2. Notice that for $k \geq 3$, the (y, λ)-projection curves of all the k-shot extremals are closed curves in the $y\lambda$-plane by the S_i, $i = 1, 2, 3$ symmetry.

Given $x_f > x(0)$, one can show that for each $n \in \mathbb{N}$ there exist exactly two n-shot extremals – one is the reflection image of the other by the S_3 symmetry – such that both produce x_f. In the case of $(1+2\alpha c) > 0$, we can prove that the two one-shot extremals are the time-optimal ones. The way of constructing them is given in § 2. However, in the case of $(1+2\alpha c) \leq 0$, we have not found any uniqueness proofs so far. Instead, we provide a finite algorithm of finding time-optimal trajectories in § 2. With this algorithm, for example, we perform a simulation with the following specification: $\alpha = -3/4, c = 1, x(0) = 1$, and $x_f = 2$. In this case, the two one-shot extremals are the optimal trajectories and the minimum time is $t_f = 7.8117$. The optimal control $u(t)$ and the optimal trajectory $(x(t), y(t))$ with $\lambda_0 = 0.8649$ are given in Figure 5.

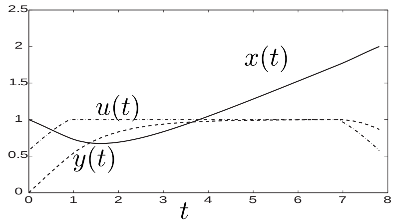

Fig. 5. Optimal solution for a sample case.

Acknowledgements. We would like to thank Bernard Bonnard, Jean Lévine, Jerry Marsden, Laurent Praly and Banavara Shashikanth for several helpful suggestions.

REFERENCES

Chang, D. E., S. Loire and I. Mezić (2003). Closed-form solutions in the electrical field analysis for dielectrophoretic and travelling wave inter-digitated electrode arrays. *J.Phys. D:Appl. Phys.* **36**(23), 3073–3078.

Hughes, M. P. (2002). *Nanoelectromechanics in Engineering and Biology.* CRC Press. Boca Raton.

Jones, T. B. (1995). *Electromechanics of Particles.* Cambridge University Press. New York.

Pohl, H. A. (1978). *Dielectrophoresis.* Cambridge University Press. Cambridge, UK.

Pontryagin, L. S., V. G. Boltyanskii, R. V. Gamkrelidze and E. F. Mishchenko (1962). *The Mathematical Theory of Optimal Processes.* John Wiley & Sons, Inc.. New York.